Angewandte Chemie
Eine Zeitschrift der Gesellschaft Deutscher Chemiker

Supporting Information

69451 Weinheim, Germany

Mechanistic Basis of Phenothiazine-Driven Inhibition of Tau Aggregation**

*Elias Akoury, Marcus Pickhardt, Michal Gajda, Jacek Biernat, Eckhard Mandelkow, and Markus Zweckstetter**

anie_201208290_sm_miscellaneous_information.pdf

Supporting Text

Impact of removal of the two cysteines on Tau aggregation. Full-length Tau has a very low tendency to aggregate, consistent with its hydrophilic nature and high solubility. The influence of cysteines can be illustrated by the following experiments: The aggregation of wild-type htau40 is observed under non-reducing conditions (i.e. omission of DTT). The reaction was monitored with Thioflavin S (Figure S2a, blue line). In the course of 8 days there is no increase of the fluorescence signal, indicating little or no aggregation. Analysis of the endpoint sample by electron microscopy revealed some occasional short filaments (Figure S2b). By contrast, when the cysteine-less htau40-mutant was monitored over the same time period, it formed abundant amounts of bundled filaments (Figures S2a, red line and S2c). This can be rationalized in the following way[1]: htau40 contains two cysteines (Cys291 and Cys322) which - in oxidative conditions - can form intra-molecular disulfide bridges that prevent dimerization and full-scale aggregation. But when the cysteine residues are replaced by alanine, aggregation can occur because the molecules are free to dimerize without the intra-molecular blocking conformation.

Next, we monitored the kinetics of aggregation of wild-type htau40 under non-reducing conditions in the presence of increasing amounts of MB by the filter assay (Figures S2d). [Note: MB interferes with the ThS fluorescence, which precludes the use of ThS fluorescence for filament detection.] The analysis showed small amounts of randomly aggregated material over the whole range of MB concentrations.

In the case of aggregation of wild-type htau40 under non-reducing conditions an inhibitory effect of MB cannot be detected because of the absence of free -SH groups (there is only minimal aggregation because of intra-molecular S-S bridges in the compact monomer conformation, see[1]). The result of the comparable experiment with the cysteine-less htau40-mutant also does not show any inhibitory effect of MB because of the lack of -SH groups. The noticeable aggregation of the htau40-mutant can be explained by the fact that this protein is able to dimerize and to form β-sheet stacking via hexapeptide motifs. In other words, intra-molecular disulfide bridges prevent aggregation (because they lock the molecule in a non-polymerizable state), inter-molecular disulfide bridges accelerate aggregation because they accelerate dimerization.

Supporting Methods

Proteins and Reagents. Unlabelled and ^{15}N-labelled wild-type and mutant human Tau proteins were expressed and purified as described previously.[2] Methylene Blue (MB), azure A and azure B were purchased from MP Biomedicals (MP Biomedicals S.A. Heidelberg, Germany). Dithiothreitol DTT and Thioflavin S were purschased from Sigma (Sigma–Aldrich Chemie GmbH, Schnelldorf, Germany). $^{13}C/^{15}N$ double-labelled cysteine was purschased from Cambridge Isotope Laboratories (Cambridge Isotope Laboratories, Andover, United States).

Quantification of aggregated Tau protein via filter-assay. 10 µM of cysteine-free Tau protein (htau40/C291A/C322A) was incubated in the presence of BES buffer (20 mM, pH 7.4), 25 mM NaCl, 2.5 µM $heparin_{3000}$, protease-inhibitor mix (10 µg/ml leupeptin, 1 µg/ml aprotinin, 1 µg/ml pepstatin, and 1 mM benzamidin). Methylene Blue or Azure B were added in a concentration range from 0 to 1 mM and the samples were incubated for 8 days at 37^0C. Tau aggregation was monitored in the compound free sample by Thioflavin S assay and electron microscopy. After incubation, 2 % of the sample were filtered through an equilibrated nitrocellulose membrane (ø 0.45 µm; Biorad, Schleicher and Schüll Bioscience GmbH, Dassel, Germany) and washed two times with 40-fold PBS buffer volume (137 mM NaCl, 2.7 mM KCl, 12 mM Na_2HPO_4/KH_2PO_4, pH 7.4). the membrane was shaken for 15 minutes in PBS to remove air bubbles ouf of the nitrocellulose matrix. The amount of remaining aggregated Tau was quantified via immunological detection with the pan-Tau antibody K9JA (anti-rabbit-goat HRP). The secondary antibody is labeled with HRP and the measurement was performed via ImageQuant LAS4000 mini (GE Healthcare), detection via ECL system (GE Healthcare), and quantification via Aida Image Analyzer software.

Electrospray Ionization Mass Spectrometry. Samples of free (100 µM) and MB–containing (equimolar) $^{13}C/^{15}N$ double-labelled cysteine amino acid (Cambridge Isotope Laboratories, Andover, United States) were dissolved in 20 % acetonitrile / 0.2 % formic acid–aqueous solutions and directly infused into a Thermofisher LTQ instrument via a syringe pump at 3 ml/min. Spectra were acquired in the positive mode in the range of 60 to 600 m/z, under the following source conditions: voltage 3.8 kV, capillary temperature 275 ^{0}C; and processed with XCalibur.

NMR Spectroscopy. All NMR experiments were recorded at 5 ^{0}C on Bruker Avance 700 MHz or Avance III 800 MHz spectrometers equipped with cryogenic probes. NMR samples contained 100 µM ^{15}N-labelled protein in 50 mM phosphate buffer pH 6.8, 1 mM DTT and 10 % (v/v) D_2O unless noted differently. 2D $^1H–^{15}N$ HSQC experiments were acquired using 600 complex points and 32 scans per increment with spectral widths of 8389 Hz and 1844 Hz in the ^1H and ^{15}N dimensions, respectively. Intensity ratio plots are reported with a 3–residues averaging window.

1D ^1H and 2D $^1H–^{13}C$ NMR spectra of the amino acid cysteine (100 µM in the absence or presence of a 20-folded excess of MB prepared in 50 mM phosphate buffer, pH 6.8 and 10 % (v/v) D_2O, were acquired at 5 ^{0}C on a Bruker 400 MHz spectrometer using 16k points, 1k scans with spectral widths of 4006 Hz (in case of 1D ^1H NMR spectra) and 144 complex points, 16 scans per increment with spectral widths of 4006 Hz and 4024 Hz in the ^1H and ^{13}C dimensions, respectively (in case of 2D $^1H–^{13}C$ NMR spectra).

NMR diffusion experiments were recorded on a Bruker Avance 600 MHz spectrometer equipped with a cryogenic probe using a stimulated–echo based pulsed gradient spin–echo sequence incorporating the WATERGATE solvent suppression [3] with optimized diffusion time and gradient pulses lengths. The gradient strength was linearly increased from 2 % to 95 % of the maximum gradient strength in 30 steps, where the 100 % gradient strength corresponds to 55.14 G/cm. Each ^1H spectrum was recorded with 128 scans and 16K complex over a spectral width of 8992 Hz. Several

peaks in the aliphatic region of htau40 were selected and the intensities of their diffusion–based spin–echo attenuation were extracted to determine an average diffusion coefficient. Stokes radii were calculated from the apparent diffusion coefficients of htau40 referenced to a selection of protein standards (cytochrome C 12.4KDa, 17.8 Å; lysozyme 14.3 KDa, 20.5 Å; myoglobin 18 KDa, 21.2 Å; and ovalbumin 45 KDa, 30.5 Å; all prepared at concentrations of 100 μM in 50 mM phosphate buffer containing 1 mM DTT and 10 % (v/v) D_2O).

Dynamic Light Scattering. DLS measurements were performed at 5 ^{0}C using a DynaPro Titan/temperature controlled microsampler (Wyatt Technologies Corporation). Samples (40 μM of htau40 in 50 mM phosphate buffer, pH 6.8 and 1 mM DTT inserted in 50 μl flow cells) were illuminated by a 25 mW, 780 nm solid–state laser, and the intensity of 90^0 angle scattered light was measured at 4 μs intervals by a solid–state avalanche photodiode. Measurements were repeated three times using freshly prepared samples to confirm the reproducibility of the results, and the average values with their standard deviations were analyzed and reported by the Dynamics 6.7.7.9 software package.

Circular Dichroism. Samples contained 10 μM htau40 in 50 mM phosphate buffer pH 6.8 and 1 mM DTT. CD spectra were acquired at room temperature using a 1–mm path cell cuvette, on a Chirascan CD spectrometer (Applied Photophysics Limited) over the range covering 190 to 250 nm and a 1 nm band width and a scanning speed of 20 nm/min. Spectra were averaged over five scans. The measurements were repeated three times with freshly prepared samples to confirm the reproducibility of the results. Data are expressed in terms of the mean residual ellipticity (θ) in deg cm^2 $dmol^{-1}$.

Small Angle X-ray Scattering. SAXS Data were collected at X33 at the European Molecular Biology Laboratory on DORIS III (DESY) at a wavelength of 1.5 Å at 25 °C using a Pilatus 1M photon counting detector. Each sample contained 87 μM (4 mg/m) of htau40 in 50 mM phosphate buffer, pH 6.8 and 1 mM DTT, and was exposed to 8 frames of 15 seconds. Data were analyzed by ATSAS 2.3.[4] The maximum diameter was estimated by indirect fourier transformation.

Supporting Figures

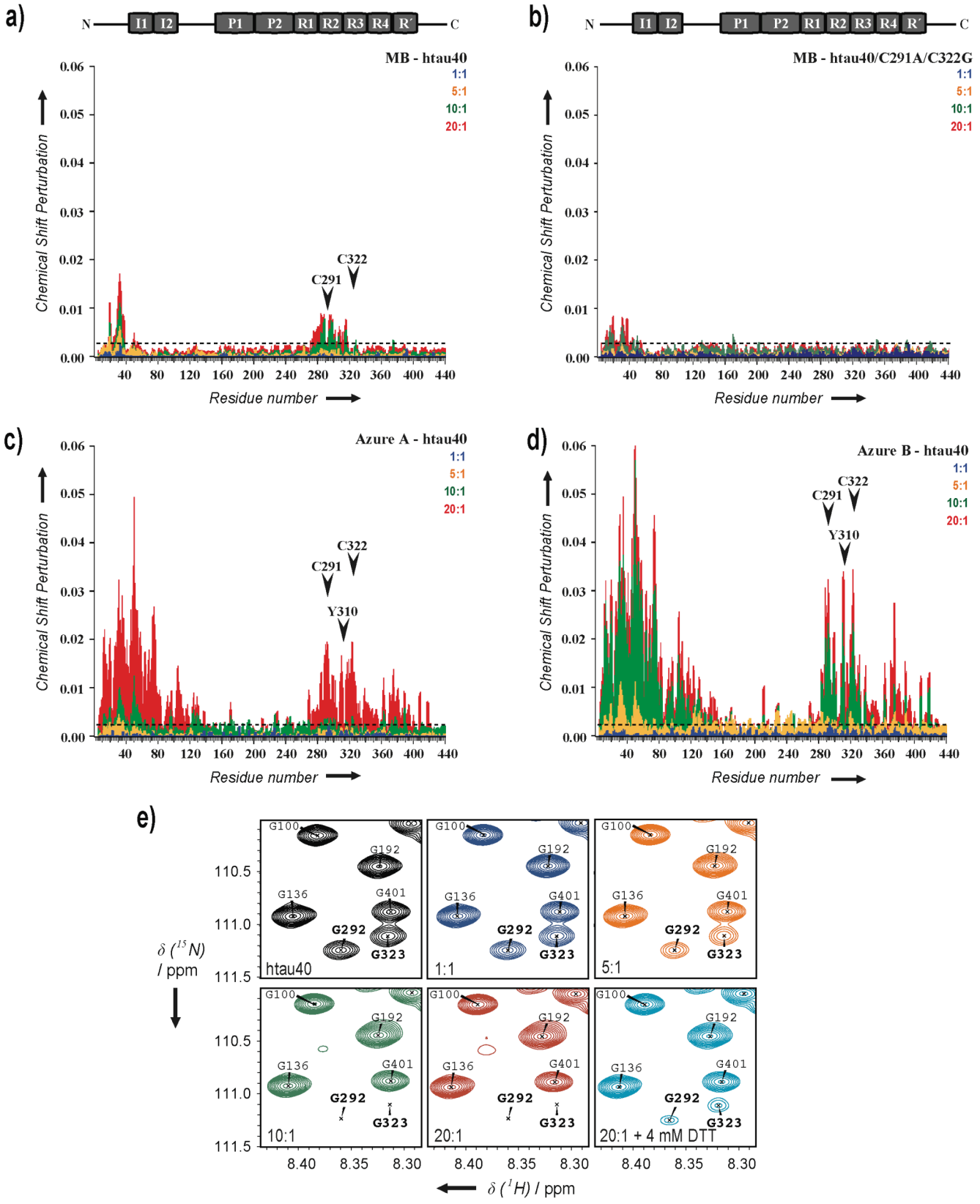

Figure S1. Chemical shift deviations ($\Delta\delta_{1H/15Ntit}-\Delta\delta_{1H/15Nref}$) observed in 2D $^{1}H–^{15}N$ HSQC NMR spectra of htau40 wild-type and mutants at increasing compound concentrations: a, b) MB, c) azure A, and d) azure B. Averaged, normalized chemical shift deviations were calculated according to $\Delta\delta_{AV}=[0.5(\delta_{Htit}-\delta_{Hwt})^2+0.02(\delta_{Ntit}-\delta_{Nwt})^2]^{½}$. Dotted black lines correspond to thresholds of chemical shift perturbations of 0.0025 ppm. e) Selected regions of 2D $^{1}H–^{15}N$ HSQC of htau40 at increasing concentrations of MB, and after further addition of 4 mM DTT (light blue).

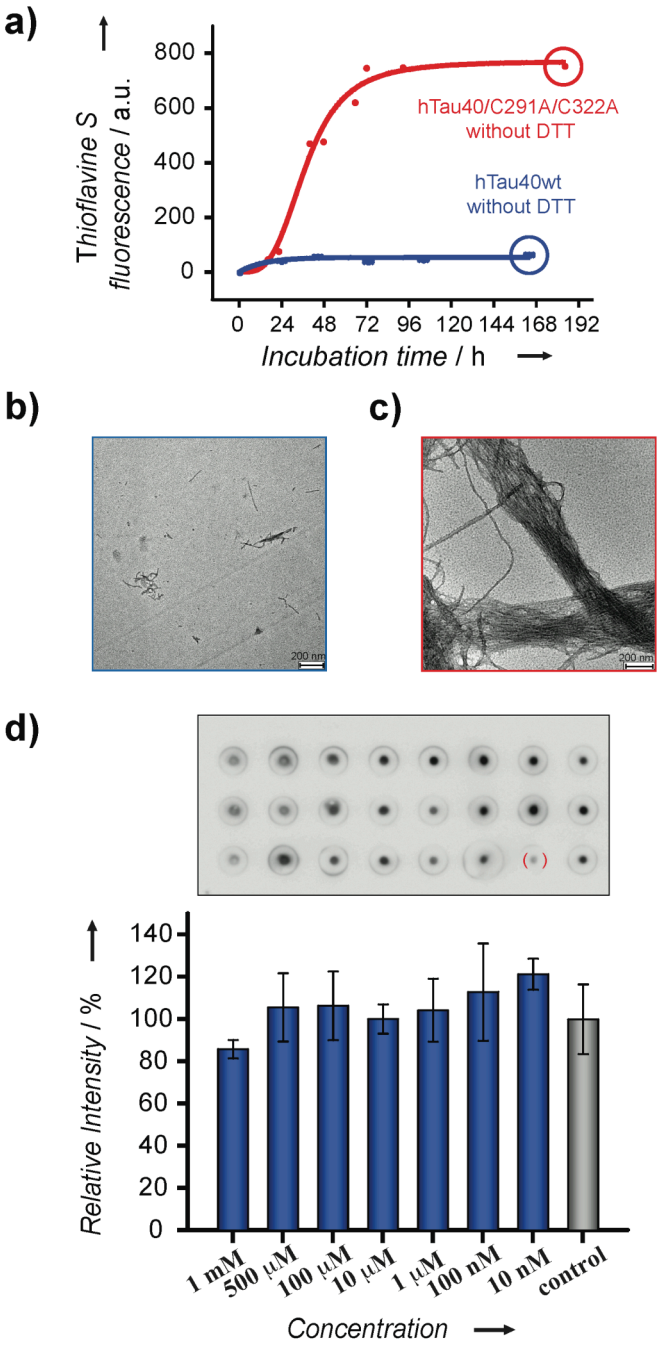

Figure S2. Impact of removal of the two native cysteines on Tau aggregation. a) Aggregation curve of wild-type htau40 (blue line) compared with the cysteine-less mutant htau40/C291A/C322A (red line) under non-reducing conditions without MB treatment monitored by a Thioflavin S assay. b, c) Endpoint samples (after 168h for wild-type htau40, blue circle and after 192h for htau40/C291A/C322A, red circle) were monitored by electron microscopy to show the amount and shape of aggregated Tau protein. d) Filter assay of aggregated wild-type htau40 in the presence of increasing amounts of MB (0 to 1 mM) (see Supporting Text for additional information).

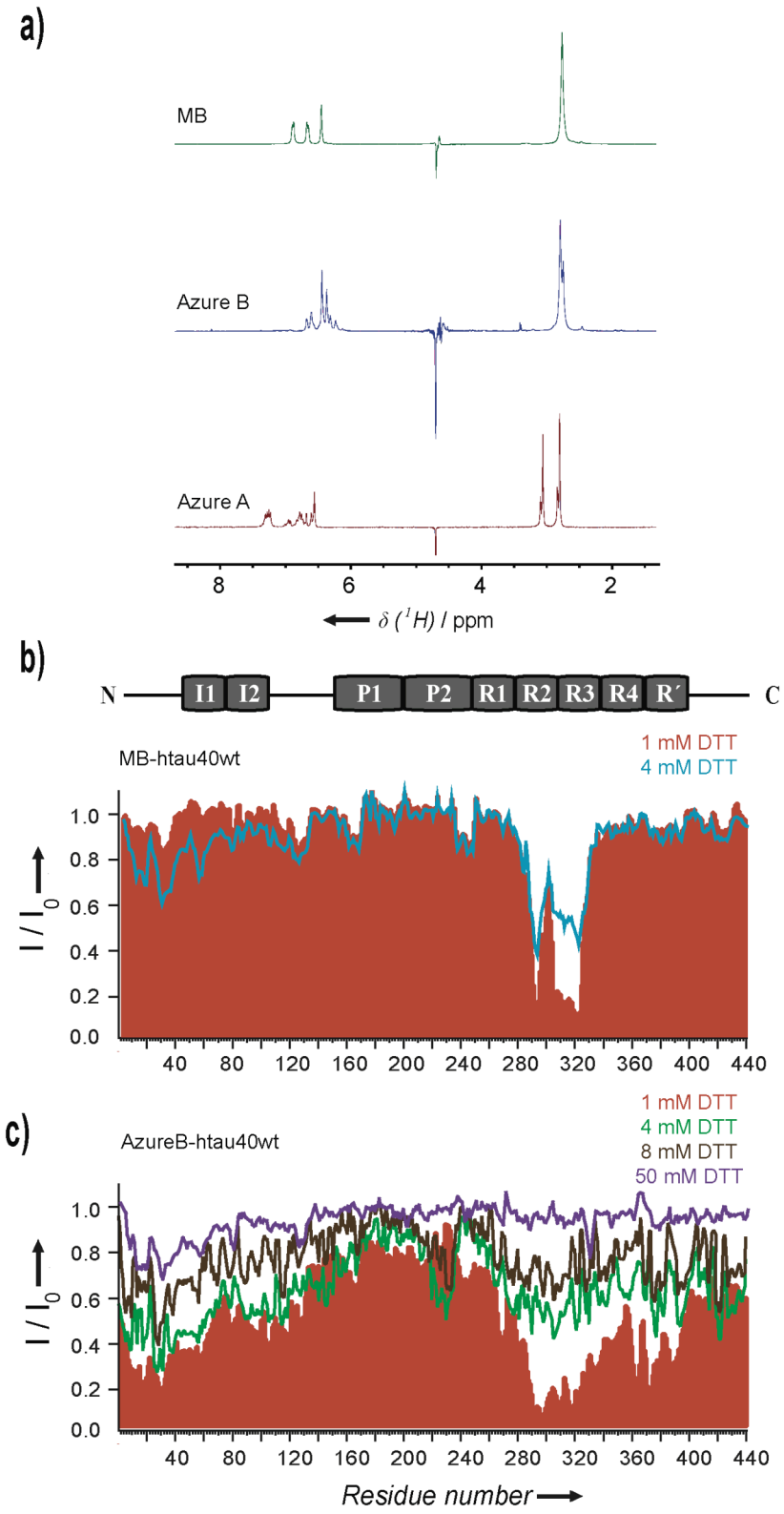

Figure S3. Interplay between oxidized and reduced forms of MB and azure B. a) 1D ^{1}H NMR spectra of MB, azure B and azure A. b) NMR signal intensity ratios in 2D ^{1}H–^{15}N HSQC of htau40 for MB–htau40 20:1 in the presence of 1 mM (red) and of 4 mM DTT (light blue). c) NMR signal intensity ratios in 2D ^{1}H–^{15}N HSQC of htau40 for azureB–htau40 20:1 in presence of 1 mM (red), 4 mM (green), 8 mM (brown) and 50 mM DTT (purple).

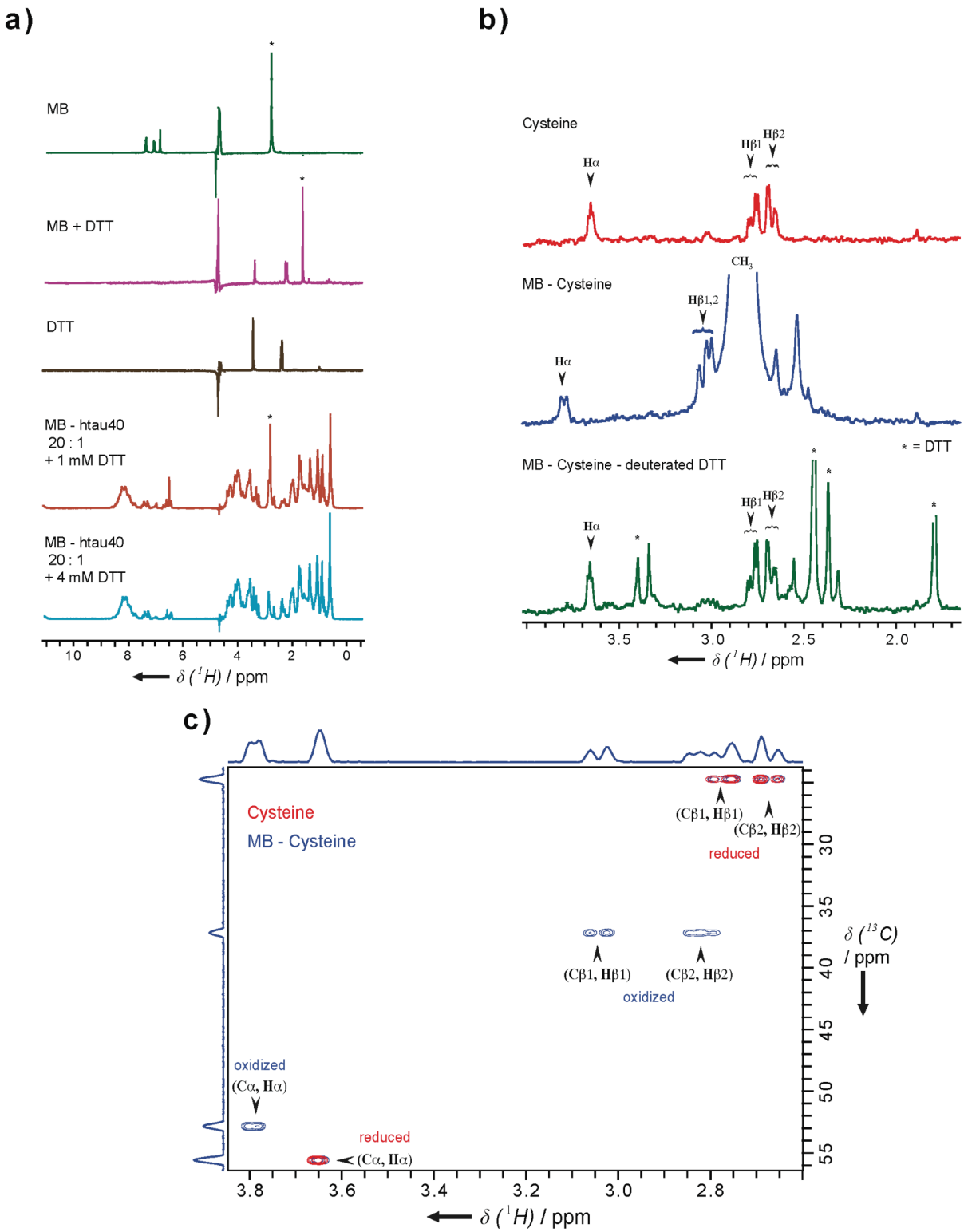

Figure S4. Reversible modification of cysteine by MB. a) 1D ^{1}H NMR spectra of selected samples to highlight the redox reaction. The oxidized form of MB is reduced in the presence of excess DTT. Upon increasing the concentration of deuterated DTT from 1 to 4 mM in the MB-htau40 sample, the concentration of oxidized MB is decreased. Note that this was also clearly visible by the change in color of the NMR sample. The sample color changed from blue (oxidized MB) to transparent (leucoMB). b) 1D ^{1}H NMR spectra of the free amino acid cysteine in absence (red) and presence of MB (blue) showing the displacement of H_α and H_β chemical shifts further downfield upon oxidation together with their recovery in presence of deuterated DTT (green). c) Superposition of 2D ^{1}H-^{13}C NMR spectra of the amino acid cysteine in the absence (red) and presence of MB (blue) showing the (C_α,H_α) and (C_β,H_β) chemical shifts in their reduced and oxidized forms.

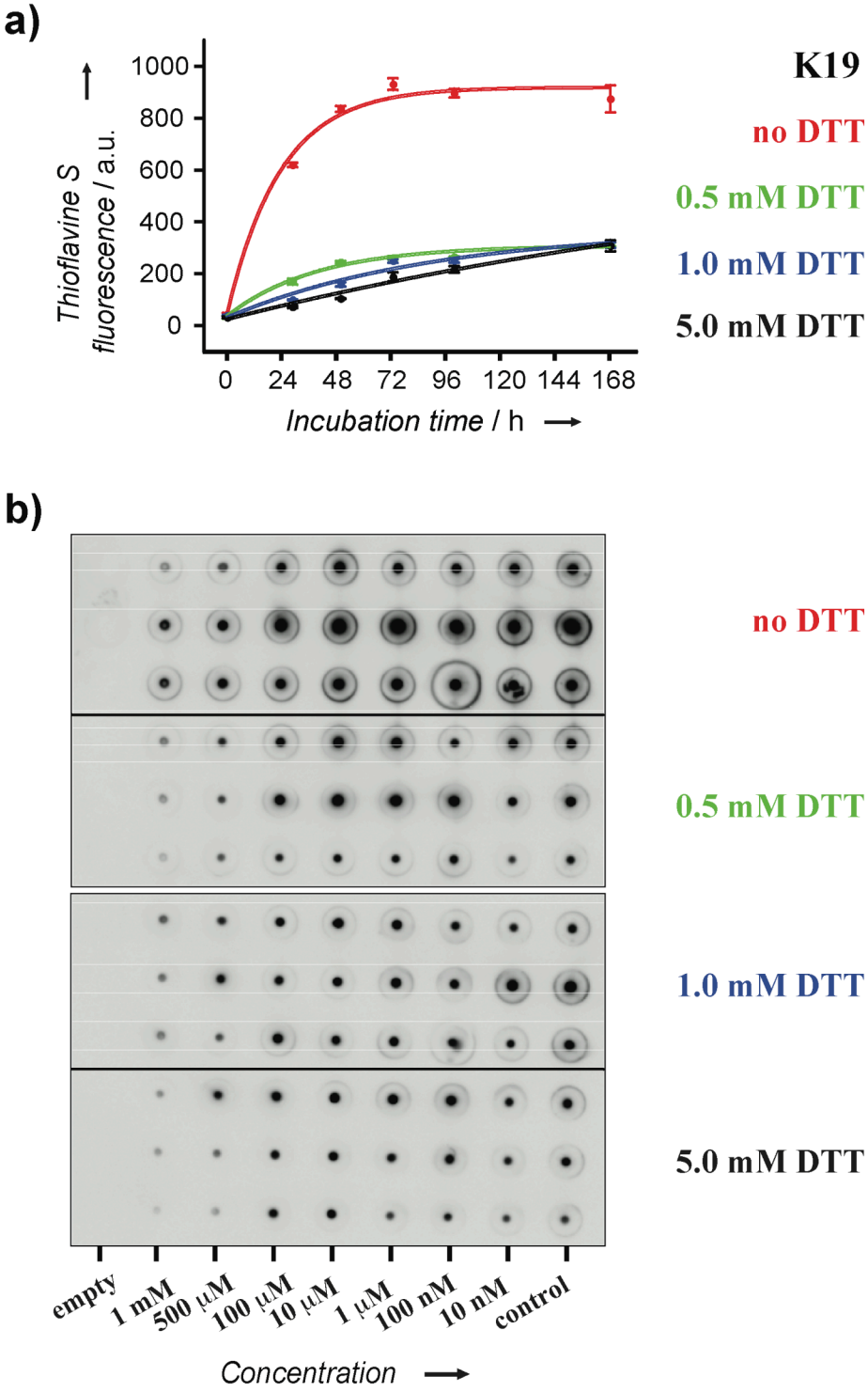

Figure S5. MB-driven inhibition of Tau aggregation under reducing conditions. a) Aggregation of the three-repeat Tau construct K19 under reducing conditions in the presence of increasing DTT concentrations but without MB as monitored by a Thioflavin S assay. b) Aggregation of K19 in the presence of different DTT and MB concentrations measured by the filter assay (see also Figure 2h and Methods in Supporting Information for further details).

Supporting References

[1] O. Schweers, E. M. Mandelkow, J. Biernat, E. Mandelkow, *Proc Natl Acad Sci U S A* **1995**, *92*, 8463-8467.

[2] M. D. Mukrasch, J. Biernat, M. von Bergen, C. Griesinger, E. Mandelkow, M. Zweckstetter, *J Biol Chem* **2005**, *280*, 24978-24986.

[3] D. H. Wu, A. D. Chen, C. S. Johnson, *J Magn Reson Ser A* **1995**, *115*, 260-264.

[4] P. V. Konarev, M. V. Petoukhov, V. V. Volkov, D. I. Svergun, *J Appl Cryst* **2006**, *39*, 277-286.